Human Brain Mapping

WILEY

RESEARCH ARTICLE OPEN ACCESS

Prediction Model and Nomogram for Amyloid Positivity Using Clinical and MRI Features in Individuals With Subjective Cognitive Decline

Qinjie Li[1] | Liang Cui[1] | Yihui Guan[2] | Yuehua Li[3] | Fang Xie[2] | Qihao Guo[1]

[1]Department of Gerontology, Shanghai Jiao Tong University Affiliated Sixth People's Hospital, Shanghai, China | [2]PET Center, Huashan Hospital, Fudan University, Shanghai, China | [3]Department of Radiology, Shanghai Jiao Tong University Affiliated Sixth People's Hospital, Shanghai, China

Correspondence: Yuehua Li (liyuehua312@163.com) | Fang Xie (fangxie@fudan.edu.cn) | Qihao Guo (qhguo@sjtu.edu.cn)

Received: 20 November 2024 | **Revised:** 10 April 2025 | **Accepted:** 17 May 2025

Funding: This study was funded by the Shanghai Jiao Tong University Affiliated Sixth People's Hospital Retrospective Study Project (ynhg202321).

Keywords: Alzheimer's disease | logistic regression | machine learning | nomogram | subjective cognitive decline

ABSTRACT

There is an urgent need for the precise prediction of cerebral amyloidosis using noninvasive and accessible indicators to facilitate the early diagnosis of individuals with the preclinical stage of Alzheimer's disease (AD). Two hundred and four individuals with subjective cognitive decline (SCD) were enrolled in this study. All subjects completed neuropsychological assessments and underwent 18F-florbetapir PET, structural MRI, and functional MRI. A total of 315 features were extracted from the MRI, demographics, and neuropsychological scales and selected using the least absolute shrinkage and selection operator (LASSO). The logistic regression (LR) model, based on machine learning, was trained to classify SCD as either β-amyloid (Aβ) positive or negative. A nomogram was established using a multivariate LR model to predict the risk of Aβ+. The performance of the prediction model and nomogram was assessed with area under the curve (AUC) and calibration. The final model was based on the right rostral anterior cingulate thickness, the grey matter volume of the right inferior temporal, the ReHo of the left posterior cingulate gyrus and right superior temporal gyrus, as well as MoCA-B and AVLT-R. In the training set, the model achieved a good AUC of 0.78 for predicting Aβ+, with an accuracy of 0.72. The validation of the model also yielded a favorable discriminatory ability with an AUC of 0.88 and an accuracy of 0.83. We have established and validated a model based on cognitive, sMRI, and fMRI data that exhibits adequate discrimination. This model has the potential to predict amyloid status in the SCD group and provide a noninvasive, cost-effective way that might facilitate early screening, clinical diagnosis, and drug clinical trials.

1 | Introduction

Alzheimer's disease (AD) is the most common cause of dementia, which has a progressive neuropathological course that spans several years to decades before the first symptom of cognitive impairment (Jack et al. 2018). According to the international consensus on the biological definition, AD is acknowledged as a continuum characterized by underlying pathologic processes (Jack et al. 2024). The progression of the neuropathological burden eventually leads to the later appearance and progression of clinical symptoms (Jack et al. 2024). Consensus on the clinical stages of the Alzheimer's continuum recognizes that subjective cognitive decline (SCD) is an indicator of transitional cognitive decline that may precede the MCI by 10–15 years, which lies between a cognitively unimpaired state and impaired cognition (Jack et al. 2018). Given its long prodromal period before the first symptom, diagnosis, and intervention measures should commence as early as possible (Sperling et al. 2014). Due to the massive loss of neurons and irreversible cognitive impairment that have already occurred at MCI, detecting at the stage of MCI

Summary

- There is an urgent need for the prediction of cerebral amyloidosis using a noninvasive method to facilitate the early diagnosis of AD.
- The prediction model we have developed and validated, based on cognitive, sMRI, and fMRI data, effectively discriminates Aβ+ in SCD with an AUC of 88%, a sensitivity of 81%, and a specificity of 85% in the test set.
- We have constructed a nomogram that holds potential for clinical reference in assessing the individual-level probability risk of Aβ+ in the brain.

may still be too late for early intervention (Petersen 2009). AD would be treated optimally in the "presymptomatic" or "preclinical" stages before detectable cognitive impairment happens (Sperling et al. 2011).

There are two broad criteria that can define SCD: a self-experienced persistent decline in cognitive capacity compared to previously normal status and unrelated to an acute event, and normal performance on standardized cognitive tests, which are used to classify MCI (Jessen et al. 2014). In addition, an open set of specific features has been proposed as SCD plus (Jessen et al. 2014), such as concerns (worries) associated with subjective cognitive decline; age at onset of subjective cognitive decline ≥ 60 years; onset of subjective cognitive decline within the last 5 years; feeling of worse performance than others of the same age group. These have previously been found to indicate an increased association with AD pathology or a particular risk of objective decline (Jessen et al. 2014). Globally, there is a high prevalence of missed diagnoses for the early stage of AD, along with poor rates of follow-up and treatment compliance (Alzheimer's disease facts and figures 2024). Sometimes, patients who come to the clinic seeking treatment already present with moderate or severe dementia and have missed the optimal time for intervention (Han et al. 2020). The early detection of individuals with AD poses a challenge in the field of research.

The current consensus emphasizes the necessity of early detection of AD, which is based on the neuropathological category of amyloid-β deposition, pathologic tau, and neurodegeneration [AT(N)] (Jack et al. 2016; Jack et al. 2018). Amyloid-β (Aβ) positron emission tomography (PET) imaging allows in vivo detection of fibrillar amyloid-β in neuritic plaques, which is a core neuropathological feature of AD. The estimated prevalence of Aβ pathology in individuals aged 60– 80 varies from 10% to 33% among cognitively normal (CN) subjects (including SCD), and from 37% to 60% in those with MCI (Jansen et al. 2015). The high cost and limited accessibility of assessing amyloid pathology through PET for screening purposes have constrained its clinical applications. The identification of noninvasive methods capable of predicting amyloid pathology has the potential to diminish reliance on invasive, costly, and time-consuming procedures, thereby significantly enhancing the efficiency of clinical assessments for the earlier detection and monitoring of patients at risk for neurodegenerative diseases associated with amyloid-related changes.

In AD progresses, as these pathological deposits accumulate, those changes may lead to neuronal dysfunction and eventual structural alterations (Wang et al. 2020). The entorhinal cortex and hippocampus, which are preferential target locations of neurofibrillary tangles (Wang et al. 2020), exhibit significant atrophy in patients with Alzheimer's disease-related dementia. Structural MRI (sMRI) is a noninvasive brain imaging technique that can detect AD-related morphological alterations, such as medial temporal lobe atrophy, in subjects with SCD. Previous structural magnetic resonance imaging studies showed that subjects with SCD have a loss of grey matter (GM) volume and/or cortical thickness in the areas of hippocampus (Flier et al. 2004; Meiberth et al. 2015; Peter et al. 2014); entorhinal cortex (Hu et al. 2019; Meiberth et al. 2015), and frontotemporal regions (Saykin et al. 2006; Wang et al. 2020). However, the stability and conclusiveness of such alterations are limited in individuals with SCD compared to those observed in studies on AD and MCI (Parker et al. 2020; Ryu et al. 2017; Sun et al. 2016), potentially due to confounds arising from differences in cross-sectional design or race, as well as sample recruitment. Resting-state functional MRI (rs-fMRI) is a noninvasive method that identifies changes in spontaneous brain activity, regional homogeneity (ReHo), and interregional functional connectivity by assessing fluctuations in low-frequency blood oxygen level-dependent (BOLD) signals, which may reflect functional deficits before the appearance of cognitive decline and brain structural atrophy (Sun et al. 2016; Zhang, Wang, et al. 2021). Accumulating evidence indicates that the amplitude of low-frequency fluctuations (ALFF) and ReHo are selectively disrupted in individuals with SCD compared to healthy controls, such as reporting a higher ALFF in the left inferior parietal lobule and right middle occipital gyrus and a lower ALFF in the posterior cingulate cortex (PCC), precuneus, and cerebellum (Sun et al. 2016; Yang et al. 2018; Zhang, Wang, et al. 2021), a decreased ReHo in the PCC (Sun et al. 2016; Zhang, Cui, et al. 2021) and an increased ReHo in caudate nucleus, temporal lobe, and the frontal lobe (Sun et al. 2016; Zhang, Cui, et al. 2021).

In recent years, a variety of machine learning methods, such as data-driven techniques, have been established to investigate strategies that may be applied in the treatment and diagnosis of AD. Unlike traditional methods that focus on several predefined regions or networks of interest, machine learning techniques are capable of fully using the rich information available in neuroimaging data. Previous studies have used machine learning methods combined with imaging data and achieved many valuable results (Pan et al. 2023; Pereiro et al. 2021). Mara and colleagues used sMRI to predict amyloid pathology, resulting in an AUC = 0.81 in MCI subjects, an AUC of 0.74 in CN subjects, and an AUC of 0.85 in the whole sample (Pereiro et al. 2021). However, there is a lack of studies utilizing MRI data to establish a prediction and nomogram model for Aβ positivity in specific individuals with SCD. Within the brain, the accumulation of pathological alterations ultimately results in both structural and functional modifications, subsequently contributing to the onset of dementia. We propose that subtle early alterations in functional and structural domains of the brain may hold significance with respect to the underlying Aβ pathology.

In this study, we evaluate the use of easily obtainable sMRI and fMRI measures combined with demographics and cognitive

assessments for the prediction of amyloid pathology in individuals with SCD. We first selected features using the least absolute shrinkage and selection operator (LASSO) regression (Tibshirani 1996; Tibshirani et al. 2005), a regularization technique commonly employed in machine learning and statistics that has proven effective for selecting the most relevant features for the response variable. Next, we used logistic regression (LR) analysis to develop a multi-variable machine learning classifier for predicting brain amyloid pathology in individuals with SCD. Moreover, to better assess the probability risk of amyloid positivity at a single subject level, a nomogram was constructed by proportionally converting each regression coefficient derived from the LR model.

2 | Methods

2.1 | Participants

A total of 204 participants (64.71% females; Mean age = 64.66 years; range: 50–84 years) were recruited from the Department of Geriatrics, Shanghai Sixth People's Hospital, and the community between April 2021 to April 2024. All participants have nearly normal eyesight and hearing to finish neuropsychological measures. Participants with history of head trauma, alcoholism, drug abuse, or other neuropsychiatric disorders that could potentially impact cognitive function were excluded. Relevant laboratory tests were carried out to exclude metabolic disorders, nutritional deficiencies, such as abnormalities in folic acid, vitamin B12, thyroid function, and treponema pallidum particle agglutination. All participants agreed to undergo AV45 PET scans and received structure magnetic resonance imaging (sMRI) and functional MRI (fMRI). This study was approved by the ethics committee of the Shanghai Sixth People's Hospital. All participants signed an informed consent.

2.2 | Neuropsychology and Diagnostic Criteria

All participants complete a comprehensive battery of neuropsychological measures, including the Chinese version of Addenbrooke's Cognitive Examination-III (ACE-III), Montreal Cognitive Assessment Basic Version (MoCA-B) (Chen et al. 2016) and domain cognitive tests (memory, language, and executive function). The domain cognitive tests included Auditory Verbal Learning Test-Huashan (AVLT-H) (Zhao et al. 2015). Boston Naming Test (BNT) (Mack et al. 1992), Animal Verbal Fluency Test (AFT) (Zhao, Guo, and Hong (2013)), Shape Trails Test Parts A (STT-A), and Trails Test Parts B (STT-B) (Zhao, Guo, Li, et al. 2013). The criteria for SCD were firstly according to the following Jessen's criteria (Jessen et al. 2014); (Jack et al. 2018) a self-experienced persistent decline in cognition (decline in memory domain must be included), which is unrelated to an acute event; (Jack et al. 2024) normal performance on standardized cognitive tests used to classify mild cognitive impairment, adjusted for age, sex, and education; secondly, meeting more than three features of SCD plus (Jessen et al. 2014), such as age at onset of subjective cognitive decline ≥ 60 years; onset of subjective cognitive decline within the last 5 years; feeling of worse performance than others of the same age group; concerns (worries) associated with subjective cognitive decline; a confirmed cognitive decline by the informants.

2.3 | 18F-Florbetapir PET Acquisition and Preprocessing

18F-florbetapir AV-45 tracer was used to quantify amyloid burden (Clark et al. 2012). The 18F-florbetapir PET scans were performed using a PET/CT system (Biograph mCT Flow PET/CT, Siemens, Erlangen, Germany) 50 min after intravenous injection of 7.4 MBq/kg (0.2 mCi/kg) of 18F-florbetapir and lasted for 20 min. The PET images were reconstructed using the filtered back projection algorithm with corrections for decay and reoriented into a standard image grid of size 168 × 168 × 148 voxels with cubic voxels measuring 2.04 × 2.04 × 1.5 mm each, along with normalization, dead time, photon attenuation, scatter, and random coincidences. Three nuclear medicine physicians, all of whom are board-certified and experienced in the field, independently visually interpreted all 18F-florbetapir PET images following the established guidelines for visual rating, ensuring blinding to any other relevant information Sabri, Seibyl, Rowe, and Barthel (2015). The qualitative assessment was based on Brain amyloid plaque load (BAPL) scores (1: no amyloid load, 2: minor amyloid load, and 3: significant amyloid load) according to the amount of 18F-florbetapir uptake observed on the lateral temporal cortex, frontal cortex, posterior cingulate cortex/precuneus, and parietal cortex. Results were interpreted into negative and positive scans (1 = negative scans, 2 and 3 = positive scans) Sabri, Seibyl, Rowe, and Barthel (2015).

2.4 | MRI Data Acquisition and Processing

Data were collected using a 3.0 Tesla scanner (SIEMENS MAGNETOM, Prisma 3.0 T, Siemens, Erlangen, Germany). Three-dimensional T1-weighted images were acquired using a magnetization-prepared rapid gradient-echo sequence in the sagittal plane with the following parameters: matrix = 320 × 320, field of view = 256 mm × 256 mm, slice thickness = 0.8 mm, voxel size = 0.8 mm × 0.8 mm × 0.8 mm, repetition time = 3000 ms, echo time = 2.56 ms, inversion time = 1100 ms, flip angle = 7°, and number of slices = 208. FreeSurfer (v.6.0.0. https://surfer.nmr.mgh.harvard.edu) was used to obtain brain cortical thickness and gray matter volume. The cortical surfaces were automatically reconstructed and segmented from the structural images using the recon-all procedures (https://surfer.nmr.mgh.harvard.edu/).

Resting-State fMRI images were collected by the following parameters: echo-planar imaging (EPI) sequence, transverse plane, repetition time = 800 ms, echo time = 37 ms, flip angle = 52°, matrix size = 112 × 112, field of view = 224 mm × 224 mm, slice number = 66 slices, slice thickness = 2 mm, and voxel size = 2 mm × 2 mm × 2 mm. The scan process obtained 488 volumes and took a total of 390.4 s. Topup (https://fsl.fmrib.ox.ac.uk/fsl/fslwiki/topup) was applied to the EPI distortion correction (Andersson et al. 2003), which was based on the FSL 5.0.9 (https://fsl.fmrib.ox.ac.uk/fsl). The images were further processed using the toolbox of Statistic Parametric Mapping 12 (SPM12, https://www.fil.ion.ucl.ac.uk/spm/software/spm12)

and the RESTplus toolkit (https://restfmri.net/forum/restplus) (Jia et al. 2019). The first 10 time points were discarded. Then, slice timing and realignment were also conducted to correct head motion (head movement: ≥3 mm or 3° were excluded). In the next step, normalization was performed with isotropic voxel size ($2\times2\times2\,mm^3$). Then, spatial smoothing was used by convolving the three-dimensional image with a three-dimensional Gaussian kernel with a full width at half maximum (FWHM) of 6 mm linear. After that, detrending processing and regression analyses were carried out to eliminate linear drift and minimize the effects of head movement, white matter signal noise, and cerebrospinal fluid signal noise. Finally, the previously generated images were filtered between 0.01 and 0.08 Hz to control noise interferences, and fALFF in the normal band was calculated. ReHo was computed via Kendall's coefficient of concordance (KCC) as a local coherence metric of BOLD signal (Zang et al. 2004), with 27 neighboring voxels without smoothing.

2.5 | Variables Selection and Machine Learning

A total of 315 features were extracted from the MRI, demographics, and neuropsychological scales data, including 62 cortical thickness measurements, 62 grey matter volumes, 90 ReHo values, 90 fALFF values, 2 global neuropsychological tests (ACE-III and MoCA-B), 6 domain neuropsychological tests (AVLT-LD, AVLT-R, STT-A, STT-B, AFT, and BNT) and 3 demographic features (age, gender, and education years). Numerous variables were collected from participants; however, not all of them were deemed useful for establishing the machine learning model. The selection of task-specific features is a crucial procedure for optimizing the performance of the model. Least absolute shrinkage and selection operator (LASSO)'s L1 regularization term helps imposing a penalty on the absolute values of the coefficients associated with each feature. This encourages sparsity in the model, effectively shrinking less important coefficients toward zero and selecting only the most informative ones (Tibshirani 1996; Tibshirani et al. 2005). Moreover, LASSO proves to be particularly useful when dealing with collinearity issues among predictor variables (Tibshirani 1996; Tibshirani et al. 2005). After that, the remaining features were used to construct a machine learning algorithm. Logistic Regression (LR) is a type of probabilistic statistical classification model that can be used to predict the classification of nominal variables based on certain features. The classification is accomplished by utilizing the logit function to evaluate the probability of outcomes. In this study, the training and test sets were randomly divided in a ratio of 2:8. Utilizing the selected optimal features, we employed LR for classification analysis. The test set was utilized to enhance the efficiency of these models.

2.6 | Statistical Analysis

Demographic and scale data for all study participants were analyzed using SPSS (version 23.0; SPSS, Chicago, III) and R 4.3.1 software (https://www.Rproject.org). The Kolmogorov–Smirnov test was used to evaluate the normality of variable distributions. For data with a normal distribution, a t-test was used to analyze the differences between groups. For data without a normal distribution, a Mann–Whitney test was performed. Continuous variables were shown as the mean with standard deviation (SD). Categorical data were presented as frequencies, and the differences between groups were examined by Chi-square test. An LR method was developed to train a machine learning model for classification of the participants with Aβ+ and Aβ−. Participants were randomly divided into a training set and a test set at a ratio of 8:2 using the R "caTools" package. Least absolute shrinkage and selection operator (LASSO) regression analysis was used for variable selection by R "glmnet" package. The error value of cross-validation is 10-fold, and the maximum number of iterations is 100. After selecting the variables in the LASSO, univariate logistic regression analysis (R "rms" package) was used to further screen the variables with clinical significance. Then, we used multivariate logistic regression analysis ("glm" function and R "rms" package) to construct the prediction model. Backward step-wise selection was applied by using the likelihood ratio test with Akaike's information criterion (AIC) as the stopping rule (Collins et al. 2015; Sauerbrei et al. 2011). The variance inflation factor (VIF) was used to diagnose the collinearity of each variable, with VIF values greater than 10 indicating severe multicollinearity. The nomogram is based on proportionally converting each regression coefficient in logistic regression to a 0–100 points scale. For clinical use of the model, the total scores of each patient were calculated based on the nomogram. "pROC" package and "reportROC" package were used for receiver operating characteristic curve (ROC) and testing the quality of the model. The "rms" package was used to draw and calculate the calibration curve, along with conducting the Hosmer-Lemeshow test using the hoslem.test function.

3 | Results

3.1 | Characteristics of the Study Population

In this study, a total of 204 participants were analyzed. The mean age of the participants was 64.66 ± 7.67 years, 132 women and 72 men. Table 1 shows the demographic and clinical characteristics of SCD with and without Aβ+. The SCD- and SCD+ did not differ in age (64.27 ± 8.04 vs. 65.07 ± 7.29), education years (12.29 ± 2.94 vs. 12.39 ± 2.80), ACE-III (81.06 ± 8.21 vs. 81.28 ± 8.59), STT-A (47.93 ± 16.13 vs. 47.43 ± 14.02), STT-B (123.10 ± 38.91 vs. 127.80 ± 43.60), AFT (17.52 ± 3.98 vs. 16.76 ± 4.05), and BNT (24.09 ± 3.39 vs. 23.76 ± 3.54). There was a significant difference in gender between SCD− and SCD+ ($p < 0.05$). The MoCA-B (25.38 ± 2.58 vs. 25.13 ± 3.24), AVLT-LD (5.58 ± 2.35 vs. 4.69 ± 2.78), AVLT-R (21.99 ± 1.55 vs. 20.79 ± 2.78) in the SCD− group were significantly higher than that in the SCD+ group (all $p < 0.05$). Table 2 summarizes the clinical and demographic characteristics of the study set in the SCD group. All participants were randomly divided 8 to 2 into a training set and a test set; no significant differences were found between those two groups.

3.2 | LASSO Regression Filtration and Development of a Prediction Model

By LASSO regression filtration, 315 features were reduced to 8 features (Figure 1A,B), including cortical thickness of right lateral orbitofrontal, right middle temporal, and right rostral

TABLE 1 | Demographic and clinical characteristics of SCD with Aβ− and Aβ+.

Characteristic	SCD− ($n=104$)	SCD+ ($n=100$)	p[a]
Age (years)	64.27, 8.04	65.07, 7.29	0.457
Sex (F/M)	75/29	57/43	<0.05
Education years	12.29, 2.94	12.39, 2.80	0.810
ACE-III	81.06, 8.21	81.28, 8.59	0.904
MoCA-B	25.38, 2.58	25.13, 3.24	<0.01
AVLT-LD	5.58, 2.35	4.69, 2.78	<0.05
AVLT-R	21.99, 1.55	20.79, 2.78	<0.001
STT-A	47.93, 16.13	47.43, 14.02	0.810
STT-B	123.10, 38.91	127.80, 43.60	0.417
AFT	17.52, 3.98	16.76, 4.05	0.178
BNT	24.09, 3.39	23.76, 3.54	0.502

Note: Data are presented as mean, SD.
Abbreviations: ACE-III, Chinese version of Addenbrooke's Cognitive Examination-III (ACE-III); AFT, Animal Verbal Fluency Test; AVLT-LD, Auditory Verbal Learning Test-Long-term delayed recall; AVLT-R, Auditory Verbal Learning Test-Recognition; BNT, Boston Naming Test; F, female; M, male; MoCA-B, Montreal Cognitive Assessment Basic; PET, Positron emission tomographySCD+, SCD with Aβ+; SCD−, SCD with Aβ−; STT-A, Shape Trails Test Parts A; STT-B, Shape Trails Test Parts B.
[a]Represents comparison between SCD and SCD+.

TABLE 2 | Demographic and clinical characteristics of the study set in SCD group.

Characteristic	Entire dataset	Training set	Test set	p[a]
No. of subjects	204	163	41	
Age (years)	64.66, 7.67	65.13, 7.43	62.73, 8.41	0.075
Sex (F/M)	132/72	107/56	25/16	0.745
Education years	12.34, 2.86	12.34, 2.90	12.36, 2.75	0.957
ACE-III	81.12, 8.28	81.05, 8.06	81.16, 8.10	0.673
MoCA-B	25.33, 2.71	25.38, 2.58	25.13, 3.24	0.598
AVLT-LD	5.14, 2.60	5.16, 2.57	5.05, 2.78	0.803
AVLT-R	21.40, 2.31	21.42, 2.41	21.33, 1.86	0.815
STT-A	47.69, 15.09	47.68, 15.17	47.70, 14.97	0.995
STT-B	125.40, 41.24	126.26, 43.49	121.90, 30.52	0.550
AFT	17.15, 4.02	17.14, 3.92	17.18, 4.48	0.961
BNT	23.93, 3.46	23.93, 3.49	23.90, 3.39	0.957
PET visual result (+/−)	100/104	79/84	21/20	0.623

Note: Data are presented as mean, SD.
[a]Represents comparison between training set and test set. In training set and test set, the baseline and clinical characteristics were basically similar.

anterior cingulate; the gray matter volume of right inferior temporal; the ReHo value of left PCG and right STG; as well as MoCA-B and AVLT-R. On logistic regression analysis using backward selection to test the independent significance of variables, with results reported as odds ratio (95% CI), right rostral anterior cingulate (0.08 [0.01, 0.39]), right inferior temporal (0.00 [0, 2.27]), left PCG (0.28 [0.08, 1.04]), right STG (0.07 [0.01, 0.48]), MoCA-B (0.85 [0.73, 1.00]), and AVLT-R (0.75 [0.62, 0.91]) (Table 3). The inclusion of these factors led to the minimization of the AIC (187.40) in the prediction model. The model that incorporated the above features was developed and presented as the nomogram (Figure 2). The calibration curve for the probability of Aβ+ in the training set and test set demonstrated good agreement between prediction and observation (Figure 3A,B). The Hosmer-Lemeshow test yielded a nonsignificant statistic in the training set and test set ($p=0.975$ and $p=0.397$, respectively), which suggested that there was no departure from perfect fit.

3.3 | Diagnostic Performance and Model Validation

The analysis results of the ROC curve were displayed (Figure 3C,D). This model yielded an AUC = 0.78 (95% CI: 0.71–0.85) to identify Aβ+ participants from Aβ− (Table 4) in the training set. The sensitivity, specificity, positive predictive value (PPV), negative predictive value (NPV), positive likelihood ratio (PLR), and negative likelihood ratio (NLR) were 0.67, 0.77, 0.74, 0.71, 2.97, and 0.43 in the training set. In the test set, the model yielded an AUC = 0.88 (95% CI: 0.78, 0.98). The sensitivity, specificity, PPV, NPV, PLR, and NLR were 0.81, 0.85, 0.85, 0.81, 5.40, and 0.23 in the test set.

4 | Discussion

In this study, we constructed and validated a machine-learning logistic regression model that could predict amyloid status in the SCD group based on a combination of cognitive, sMRI-based, and fMRI-based data. The AUC was 88% in the test set, with a sensitivity of 81% and specificity of 85% for discriminating amyloid positivity in SCD. Additionally, we have established a nomogram that holds potential for clinical reference in assessing the individual-level probability risk of Aβ+ in the brain. These results are of interest to clinicians as they can inform decisions regarding patient enrollment in clinical trials and facilitate the development of a valuable tool for evaluating the likelihood of amyloid deposits in patients, which is beneficial for clinical decision-making.

The AUC of 88%, accuracy of 83%, sensitivity of 81%, and specificity of 85% obtained in the test set were comparable to those

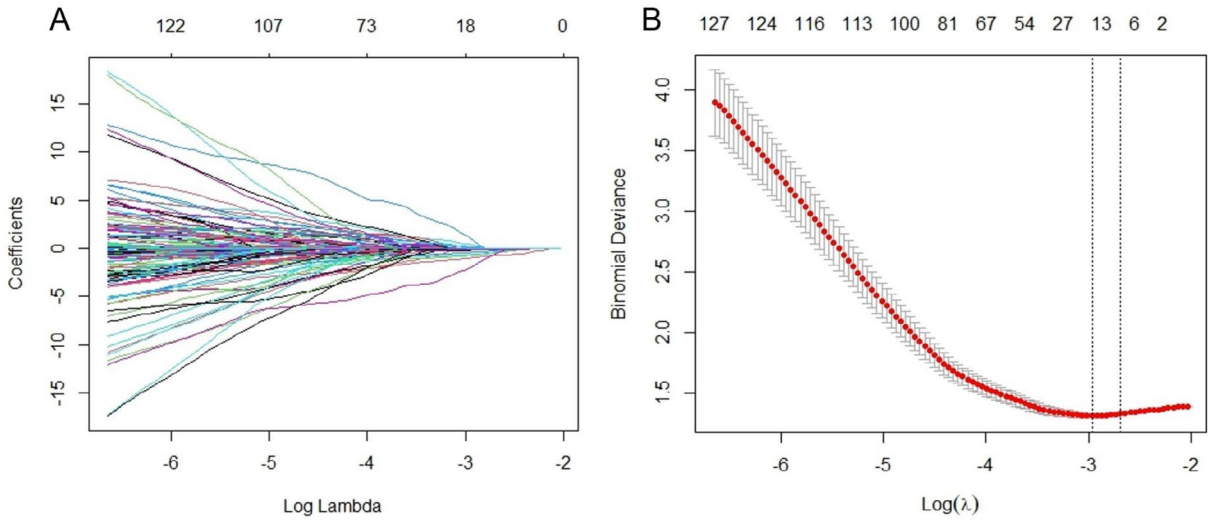

FIGURE 1 | Features selection by least absolute shrinkage and selection operator (LASSO). (A) A coefficient profile plot was produced against the log lambda sequence. LASSO coefficients profiles (y-axis) of the 12 features. (B) Ten-fold cross-validation for tuning parameter selection in the LASSO model. The partial likelihood deviance (binomial deviance) curve was plotted versus log(λ). To avoid overfitting, 1 standard error was selected.

TABLE 3 | Multivariate Logistic Regression Analysis in the training set.

Variable	β	OR (95% CI)	*p*	VIF value
rh_rostralanteriorcingulate	−2.58	0.08 (0.01, 0.39)	0.002	1.18
inferiortemporal_R	−6.23	0.00 (0, 2.27)	0.083	1.03
ReHo_PCG_L	−1.26	0.28 (0.08, 1.04)	0.057	1.15
ReHo_STG_R	−2.68	0.07 (0.01, 0.48)	0.007	1.06
MoCA-B	−0.16	0.85 (0.73, 1.00)	0.046	1.20
AVLT-R	−0.29	0.75 (0.62, 0.91)	0.004	1.24

Note: rh_rostralanteriorcingulate: mean thickness of rostral anterior cingulate in the right hemisphere; inferiortemporal_R: the gray matter volume of right inferior temporal; ReHo_PCG_L: the ReHo value of left posterior cingulate gyrus; ReHo_STG_R: the ReHo value of right superior temporal gyrus; OR: odds ratio; CI: confidence interval; VIF: variance inflation factor. Backward step-wise selection was applied by using the likelihood ratio test with Akaike's information criterion (AIC) as the stopping rule. AIC = 187.40.

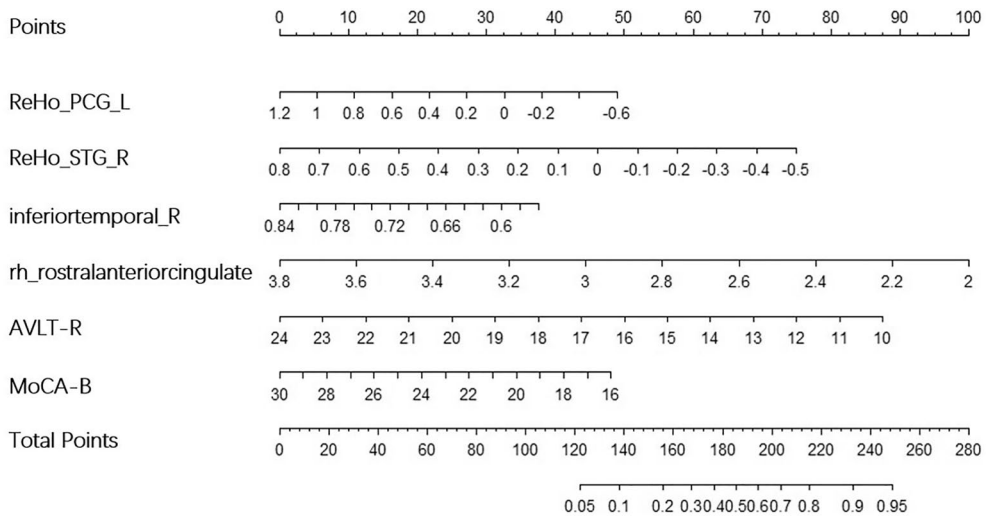

FIGURE 2 | Nomogram for the prediction model. The nomogram was developed in the training set. For instance, with the help of the nomogram model, we can see that a person with a ReHo_PCG_L value of 0.8, a ReHo_STG_R value of 0.3, an inferiortemporal_R value of 0.84, a rh_rostralanteriorcingulate value of 2.2, an AVLT-R score of 17, and a MoCA-B score of 16, might have approximately an 83% chance of Aβ+.

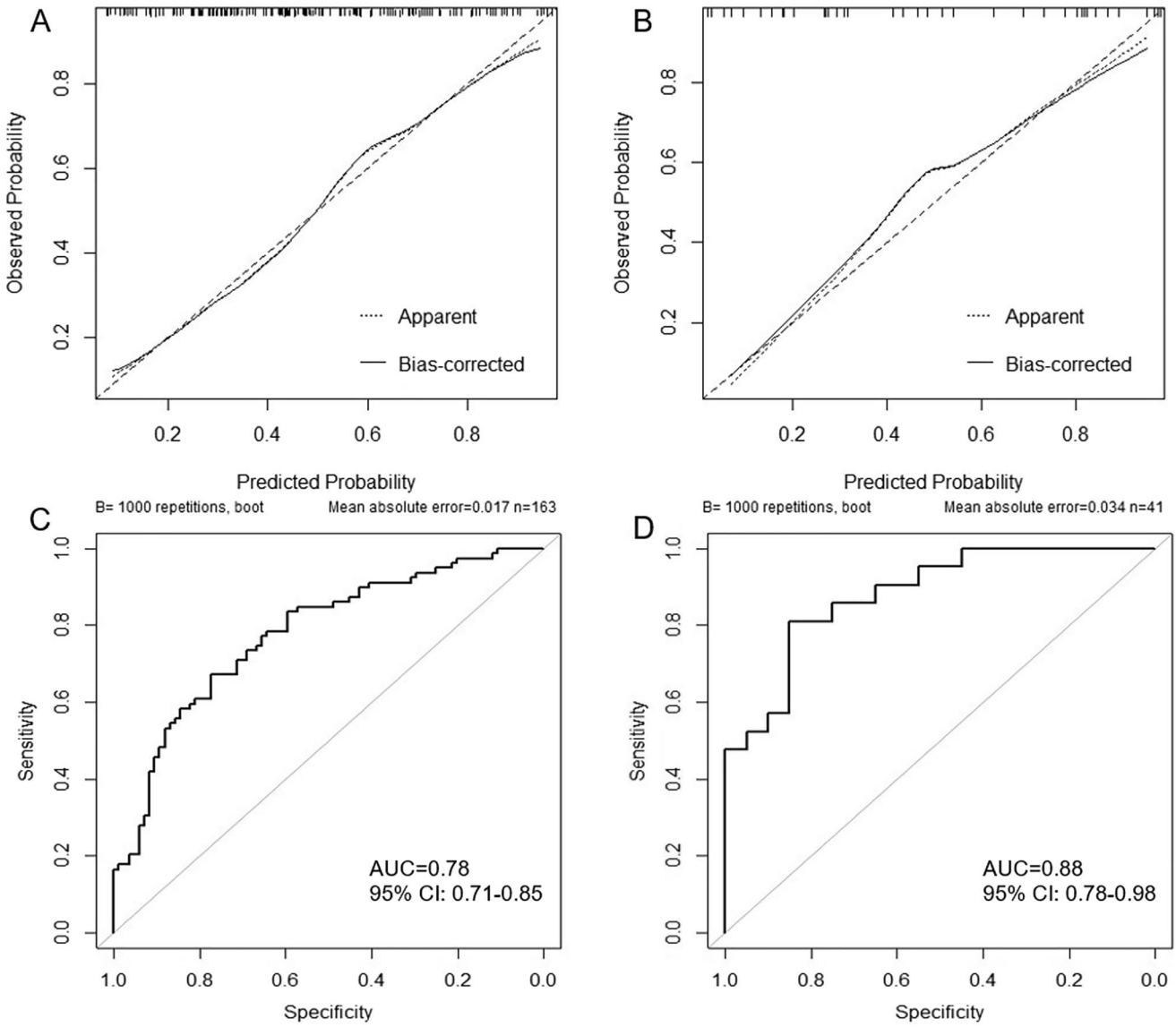

FIGURE 3 | The calibration curves of the model in the training set (A) and test set (B), and ROC curves of the prediction model in training (C) and test (D) groups. A: Training set; B: Test set; C: Training set; D: Test set. Calibration curve: The black solid line above the x-axis represents sample distribution. The dotted lines on the diagonal represent the perfect prediction of the ideal model, and the solid lines represent the performance of the training set and the test set. The closer the solid line is to the dotted line, the better the predictive effect. The x-axis represents the predicted Aβ positive risk, and the y-axis represents the actual Aβ status.

reported in previously published studies on the prediction of amyloid pathology in cognitively unimpaired subjects based on sMRI and fMRI data (Li et al. 2022; Li et al. 2023; Mehdipour Ghazi et al. 2024; Momota et al. 2024; Petrone et al. 2019; Ten et al. 2018; Tosun et al. 2021; Zhuang et al. 2024), some of which were validated using global public datasets, such as ADNI dataset (Li et al. 2023; Tosun et al. 2021; Zhuang et al. 2024). The models employed in those studies, some of which exclusively utilized structural magnetic resonance data, while others incorporated diffusion-weighted imaging (DWI) or a combination with clinical data, had an AUC of machine learning models for predicting amyloid positivity in cognitively normal elders that ranged from 0.67 to 0.90 (Mehdipour Ghazi et al. 2024; Momota et al. 2024; Petrone et al. 2019; Ten et al. 2018; Zhuang et al. 2024). The models employed fMRI data for predicting amyloid positivity; the accuracy of these models ranged from 64.3% to 78.8% (Li et al. 2022; Li et al. 2023). The machine learning models using imaging data may potentially exhibit superior performance compared to the models utilizing demographics (age, sex, education, race, family history, body mass index, marital status, and ethnicity), cognitive measures (free recall, ACE-III, immediate recall, digit symbol substitution, and delayed logical memory scores), and risk factors (APOE4 status), which exhibited an AUC that ranged from 0.60 to 0.73 (Petersen et al. 2022).

After performing variable selection using LASSO, demographic variables were excluded, while cognitive scales and MRI variables were retained. The variables included the cortical thickness of the right rostral anterior cingulate, the grey matter volume of the right inferior temporal, the ReHo values of the left posterior cingulate gyrus (PCG) and right superior temporal gyrus (STG), as well as MoCA-B and AVLT-R. The high AUC

TABLE 4 | Accuracy of the prediction of the Nomogram.

Variable	Value (95% CI)	
	Training set	Test set
Area under curve	0.78 (0.71, 0.85)	0.88 (0.78, 0.98)
Accuracy	0.72 (0.72, 0.73)	0.83 (0.82, 0.84)
Sensitivity	0.67 (0.57, 0.78)	0.81 (0.64, 0.98)
Specificity	0.77 (0.68, 0.86)	0.85 (0.69, 1.00)
Positive predictive value	0.74 (0.63, 0.84)	0.85 (0.69, 1.01)
Negative predictive value	0.71 (0.62, 0.81)	0.81 (0.64, 0.98)
Positive likelihood ratio	2.97 (1.94, 4.54)	5.40 (1.86, 15.64)
Negative likelihood ratio	0.43 (0.30, 0.60)	0.23 (0.09, 0.55)

value obtained for the cognitive measures, as well as the structural and functional variables in individuals with SCD, suggests that early-stage amyloid-related neurodegeneration in AD may be correlated with subtle changes in brain structure, function, and neuropsychological measures.

In the early stages of the disease, functional alterations may precede structural changes in the brain. ReHo reflects local neural activity by demonstrating synchronization of the BOLD signal, which can be disrupted by pathological Aβ deposits leading to functional impairments in the brain. Previous imaging studies have revealed significant atrophy or reduced cortical thickness in the ITG, ACC, and PCG regions among individuals with MCI or SCD (Guerrier et al. 2018; Jones et al. 2005; Lim et al. 2019; Wu et al. 2023). The cingulate cortex, located on the medial surface of the brain, is a structurally and functionally heterogeneous region. It can be further divided into two distinct sub-regions: the anterior cingulate (ACC) and posterior cingulate (PCC) cortex. The ACC is potentially involved in cognitive control; the reduction of awareness in AD, the rACC, and PCC areas have been verified to be susceptible to neuropathological alterations and cerebral Aβ deposition associated with AD (Kautzky et al. 2018; Sheline et al. 2010). The STG serves as the auditory language center, which can result in receptive aphasia if it gets damaged. Prior research has indicated that the STG is among the brain regions impacted by MCI and the early stages of AD (Ding et al. 2009); it plays a crucial role in encoding episodic memory, comprehending language, and processing speech. Multiple studies have reported that a decreased ReHo in the STG was found in individuals with MCI (Liu et al. 2021; Luo et al. 2018), and the ReHo value of the STG exhibited a correlation with Aβ level (Luo et al. 2018).

In our study, the model was constructed by integrating neuropsychological measurements (MoCA-B and AVLT-R) with imaging indicators through a feature selection process, thereby enhancing the predictive efficacy beyond sole reliance on neuropsychological scales as compared to the previous study (Petersen et al. 2022). In the stage of SCD, individuals typically exhibit intact cognitive abilities and function normally in their daily lives. The diagnosis of SCD does not rely on neuropsychological measurements, which primarily serve to exclude MCI. However, in individuals with SCD, more than half of the population may indicate concurrent objective cognitive decline on neuropsychological assessments, which does not reach the criterion for MCI (Cheng et al. 2023). This type of subtle cognitive decline has been demonstrated to be associated with future amyloid accumulation and neurodegeneration (Thomas et al. 2020). When we do not assess the AD-related biomarkers in elders, it is difficult to distinguish whether the subtle cognitive decline on neuropsychological measurements is age-related or AD-related. We propose that detectable cognitive decline may arise from the accumulation of subtle structural or functional changes within the brain. The composite model integrates objective neuropsychological assessments and subtle neuroimaging information, although these indicators may not possess significant independent value during the early stages of the disease.

Assessment of disease stages is crucial for determining plans of treatment and therapeutic intervention. Following SCD, individuals do not exhibit significant neurological complications or physical symptoms. Recently, the emergence of immunotherapies targeting Aβ and disease-modifying therapies (DMTs) such as Lecanemab, Aducanumab, and Donanemab offers renewed hope for patients with Alzheimer's disease (AD). Accurate and timely diagnosis of AD-related SCD would facilitate early intervention in the progression of the disease. Nomograms have gained significant popularity in the medical field due to their ability to integrate multiple risk factors and accurately predict medical outcomes and prognosis. This study demonstrated that the novel nomogram performed well in predicting Aβ+ in individuals with SCD, which is promising as a noninvasive method for identifying individuals at high risk of Aβ+.

Although there have been some excellent reports on the prediction of Aβ positivity using machine learning methods in elders with cognitively unimpaired (Long et al. 2022; Petersen et al. 2022; Petrone et al. 2019), to our knowledge, there is a paucity of literature utilizing MRI data and presenting a nomogram model for predicting Aβ positivity in specific individuals with SCD. There were several limitations in this study. Firstly, the determination of Aβ positivity was solely based on amyloid-PET scan results; however, in the preclinical stage, CSF Aβ analysis may provide enhanced sensitivity according to one recent study (Jansen et al. 2022). Second, the accuracy of machine learning is expected to be influenced by the quantity of available samples. However, our investigation was limited by a small sample size. Therefore, future research efforts will require larger sample sizes and the inclusion of independent test datasets. Third, potential selection bias was inevitable in retrospective analysis; although the cross-sectional design enabled modeling of the relationships between biomarkers performed at a single time, longitudinal follow-up data might enhance model performance. Fourth, the results of cognitive tests may be influenced by certain subjective factors, such as educational attainment, health status, and affective state. The participants selected for this study did not have severe comorbidities or family histories. Our model may not be applicable to elders with serious medical conditions or emotional problems. Fifth, our samples were obtained from one cohort in a single center, and the use of the same PET-CT and MRI scanner may potentially lead to overfitting for establishing

the model. The AUC is 88%, accuracy is 83%, sensitivity is 81%, and specificity is 85%.

5 | Conclusion

In this study, we established and validated a machine-learning logistic regression model in individuals with SCD based on demographics, cognitive, sMRI, and fMRI-based data, which could predict amyloid status in a Chinese cohort. Our model achieved 83% accuracy to predict Aβ-positivity in the brain, with an AUC of 88%, sensitivity of 81%, and specificity of 85% in the test set. Notably, we have constructed a nomogram that holds potential for clinical reference in assessing the individual-level probability risk of Aβ+ in the brain. This noninvasive and easily accessible method may have numerous applications, including aiding in the early identification of potential AD patients, facilitating enrollment in Alzheimer's disease drug clinical trials, monitoring individuals at high risk of Aβ+ development, and assessing the effectiveness of Alzheimer's disease treatments. The preliminary findings support the necessity for further multicenter investigations utilizing noninvasive imaging features to predict Aβ status in future studies.

Acknowledgments

We thank Jie-Hua Zhu, Xian-Qing Xie, and Yun Yang for their help with neuropsychological tests. Our study was supported by the fund from the Retrospective Study Project of Shanghai Jiao Tong University Affiliated Sixth People's Hospital (ynhg202321).

Conflicts of Interest

The authors declare no conflicts of interest.

Data Availability Statement

The data that support the findings of this study are available from the corresponding author upon reasonable request.

References

Alzheimer's disease facts and figures. 2024. "2024 Alzheimer's Disease Facts and Figures." *Alzheimer's & Dementia* 20, no. 5: 3708–3821.

Andersson, J. L. R., S. Skare, and J. Ashburner. 2003. "How to Correct Susceptibility Distortions in Spin-Echo Echo-Planar Images: Application to Diffusion Tensor Imaging." *NeuroImage* 20, no. 2: 870–888.

Chen, K., Y. Xu, A. Chu, et al. 2016. "Validation of the Chinese Version of Montreal Cognitive Assessment Basic for Screening Mild Cognitive Impairment." *Journal of the American Geriatrics Society* 64, no. 12: 14530.

Cheng, G., D. Liu, L. Huang, et al. 2023. "Prevalence and Risk Factors for Subjective Cognitive Decline and the Correlation With Objective Cognition Among Community-Dwelling Older Adults in China: Results From the Hubei Memory and Aging Cohort Study." *Alzheimer's & Dementia* 19, no. 11: 5074–5085.

Clark, C. M., M. J. Pontecorvo, T. G. Beach, et al. 2012. "Cerebral PET With Florbetapir Compared With Neuropathology at Autopsy for Detection of Neuritic Amyloid-β Plaques: A Prospective Cohort Study." *Lancet Neurology* 11, no. 8: 669–678.

Collins, G. S., J. B. Reitsma, D. G. Altman, and K. G. M. Moons. 2015. "Transparent Reporting of a Multivariable Prediction Model for Individual Prognosis or Diagnosis (TRIPOD): The TRIPOD Statement." *Circulation* 131, no. 2: 211–219.

Ding, S. L., G. W. Van Hoesen, M. D. Cassell, and A. Poremba. 2009. "Parcellation of Human Temporal Polar Cortex: A Combined Analysis of Multiple Cytoarchitectonic, Chemoarchitectonic, and Pathological Markers." *Journal of Comparative Neurology* 514, no. 6: 595–623.

Flier, W., M. Buchem, A. E. Weverling-Rijnsburger, et al. 2004. "Memory Complaints in Patients With Normal Cognition Are Associated With Smaller Hippocampal Volumes." *Journal of Neurology* 251, no. 6: 671–675.

Guerrier, L., J. Le Men, A. Gane, et al. 2018. "Involvement of the Cingulate Cortex in Anosognosia: A Multimodal Neuroimaging Study in Alzheimer's Disease Patients." *Journal of Alzheimer's Disease* 65, no. 2: 443–453.

Han, Z., L. Shuai, G. Jing-Huan, et al. 2020. "Analysis of Clinical Treatment of Alzheimer's Disease." *China Journal of Alzheimer's Disease and Related Disorders* 3, no. 1: 25–30.

Hu, X., C. E. Teunissen, A. Spottke, et al. 2019. "Smaller Medial Temporal Lobe Volumes in Individuals With Subjective Cognitive Decline and Biomarker Evidence of Alzheimer's Disease-Data From Three Memory Clinic Studies." *Alzheimer's & Dementia* 15, no. 2: 185–193.

Jack, C. R., J. S. Andrews, T. G. Beach, et al. 2024. "Revised Criteria for Diagnosis and Staging of Alzheimer's Disease: Alzheimer's Association Workgroup." *Alzheimer's & Dementia* 20, no. 8: 5143–5169.

Jack, C. R., D. A. Bennett, K. Blennow, et al. 2018. "NIA-AA Research Framework: Toward a Biological Definition of Alzheimer's Disease." *Alzheimer's & Dementia* 14, no. 4: 535–562.

Jack, C. R., D. A. Bennett, K. Blennow, et al. 2016. "A/T/N: An Unbiased Descriptive Classification Scheme for Alzheimer Disease Biomarkers." *Neurology* 87, no. 5: 539–547.

Jansen, W. J., O. Janssen, B. M. Tijms, et al. 2022. "Prevalence Estimates of Amyloid Abnormality Across the Alzheimer Disease Clinical Spectrum." *JAMA Neurology* 79, no. 3: 228–243.

Jansen, W. J., R. Ossenkoppele, D. L. Knol, et al. 2015. "Prevalence of Cerebral Amyloid Pathology in Persons Without Dementia." *JAMA* 313, no. 19: 1924.

Jessen, F., R. E. Amariglio, M. van Boxtel, et al. 2014. "A Conceptual Framework for Research on Subjective Cognitive Decline in Preclinical Alzheimer's Disease." *Alzheimer's & Dementia* 10, no. 6: 844–852.

Jia, X., J. Wang, H. Sun, et al. 2019. "RESTplus: An Improved Toolkit for Resting-State Functional Magnetic Resonance Imaging Data Processing." *Science Bulletin* 64, no. 14: 953–954.

Jones, B. F., J. Barnes, H. B. M. Uylings, et al. 2005. "Differential Regional Atrophy of the Cingulate Gyrus in Alzheimer Disease: A Volumetric MRI Study." *Cerebral Cortex* 16, no. 12: 1701–1708.

Kautzky, A., R. Seiger, A. Hahn, et al. 2018. "Prediction of Autopsy Verified Neuropathological Change of Alzheimer's Disease Using Machine Learning and MRI." *Frontiers in Aging Neuroscience* 10: 406.

Li, C., M. Liu, J. Xia, et al. 2022. "Predicting Brain Amyloid-β PET Grades With Graph Convolutional Networks Based on Functional MRI and Multi-Level Functional Connectivity." *Journal of Alzheimer's Disease* 86, no. 4: 1679–1693.

Li, C., M. Liu, J. Xia, et al. 2023. "Individualized Assessment of Brain Aβ Deposition With fMRI Using Deep Learning." *IEEE Journal of Biomedical and Health Informatics* 27, no. 11: 5430–5438.

Lim, E. Y., Y. S. Shim, Y. J. Hong, S. Y. Ryu, A. H. Cho, and D. W. Yang. 2019. "Different Cortical Thinning Patterns Depending on Their Prognosis in Individuals With Subjective Cognitive Decline." *Dementia and Neurocognitive Disorders* 18, no. 4: 113–121.

Liu, L., H. Jiang, D. Wang, and X. Zhao. 2021. "A Study of Regional Homogeneity of Resting-State Functional Magnetic Resonance Imaging in Mild Cognitive Impairment." *Behavioural Brain Research* 402: 113103.

Long, J. M., D. W. Coble, C. Xiong, et al. 2022. "Preclinical Alzheimer's Disease Biomarkers Accurately Predict Cognitive and Neuropathological Outcomes." *Brain* 145, no. 12: 4506–4518.

Luo, X., Y. Jiaerken, P. Huang, et al. 2018. "Alteration of Regional Homogeneity and White Matter Hyperintensities in Amnestic Mild Cognitive Impairment Subtypes Are Related to Cognition and CSF Biomarkers." *Brain Imaging and Behavior* 12, no. 1: 188–200.

Mack, W. J., D. M. Freed, B. W. Williams, and V. W. Henderson. 1992. "Boston Naming Test: Shortened Versions for Use in Alzheimer's Disease." *Journal of Gerontology* 47, no. 3: P154–P158.

Mehdipour Ghazi, M., P. Selnes, S. Timón-Reina, et al. 2024. "Comparative Analysis of Multimodal Biomarkers for Amyloid-Beta Positivity Detection in Alzheimer's Disease Cohorts." *Frontiers in Aging Neuroscience* 16: 1345417.

Meiberth, D., L. Scheef, S. Wolfsgruber, et al. 2015. "Cortical Thinning in Individuals With Subjective Memory Impairment." *Journal of Alzheimer's Disease* 45, no. 1: 139–146.

Momota, Y., S. Bun, J. Hirano, et al. 2024. "Amyloid-β Prediction Machine Learning Model Using Source-Based Morphometry Across Neurocognitive Disorders." *Scientific Reports* 14, no. 1: 7633.

Sabri, O., J. Seibyl, C. Rowe, and H. Barthel. 2015. "Beta-Amyloid Imaging With Florbetaben." *Clinical and Translational Imaging* 3, no. 1: 13–26.

Pan, F., Y. Huang, X. Cai, et al. 2023. "Integrated Algorithm Combining Plasma Biomarkers and Cognitive Assessments Accurately Predicts Brain β-Amyloid Pathology." *Communications Medicine* 3, no. 1: 65.

Parker, A. F., C. M. Smart, V. Scarapicchia, and J. R. Gawryluk. 2020. "Identification of Earlier Biomarkers for Alzheimer's Disease: A Multimodal Neuroimaging Study of Individuals With Subjective Cognitive Decline." *Journal of Alzheimer's Disease* 77, no. 3: 1067–1076.

Pereiro, A. X., S. Valladares-Rodríguez, A. Felpete, et al. 2021. "Relevance of Complaint Severity in Predicting the Progression of Subjective Cognitive Decline and Mild Cognitive Impairment: A Machine Learning Approach." *Journal of Alzheimer's Disease* 82, no. 3: 1229–1242.

Peter, J., L. Scheef, A. Abdulkadir, et al. 2014. "Gray Matter Atrophy Pattern in Elderly With Subjective Memory Impairment." *Alzheimer's & Dementia* 10, no. 1: 99–108.

Petersen, K. K., R. B. Lipton, E. Grober, C. Davatzikos, R. A. Sperling, and A. Ezzati. 2022. "Predicting Amyloid Positivity in Cognitively Unimpaired Older Adults." *Neurology* 98, no. 24: 00553.

Petersen, R. C. 2009. "Early Diagnosis of Alzheimer's Disease: Is MCI Too Late?" *Current Alzheimer Research* 6, no. 4: 324–330.

Petrone, P. M., A. Casamitjana, C. Falcon, et al. 2019. "Prediction of Amyloid Pathology in Cognitively Unimpaired Individuals Using Voxel-Wise Analysis of Longitudinal Structural Brain MRI." *Alzheimer's Research & Therapy* 11, no. 1: 72.

Ryu, S. Y., E. Y. Lim, S. Na, et al. 2017. "Hippocampal and Entorhinal Structures in Subjective Memory Impairment: A Combined MRI Volumetric and DTI Study." *International Psychogeriatrics* 29, no. 5: 785–792.

Sauerbrei, W., A. Boulesteix, and H. Binder. 2011. "Stability Investigations of Multivariable Regression Models Derived From Low- and High-Dimensional Data." *Journal of Biopharmaceutical Statistics* 21, no. 6: 1206–1231.

Saykin, A. J., H. A. Wishart, L. A. Rabin, et al. 2006. "Older Adults With Cognitive Complaints Show Brain Atrophy Similar to That of Amnestic MCI." *Neurology* 67, no. 5: 834–842.

Sheline, Y. I., M. E. Raichle, A. Z. Snyder, et al. 2010. "Amyloid Plaques Disrupt Resting State Default Mode Network Connectivity in Cognitively Normal Elderly." *Biological Psychiatry* 67, no. 6: 584–587.

Sperling, R., E. Mormino, and K. Johnson. 2014. "The Evolution of Preclinical Alzheimer's Disease: Implications for Prevention Trials." *Neuron* 84, no. 3: 608–622.

Sperling, R. A., P. S. Aisen, L. A. Beckett, et al. 2011. "Toward Defining the Preclinical Stages of Alzheimer's Disease: Recommendations From the National Institute on Aging-Alzheimer's Association Workgroups on Diagnostic Guidelines for Alzheimer's Disease." *Alzheimer's & Dementia* 7, no. 3: 280–292.

Sun, Y., Z. Dai, Y. Li, et al. 2016. "Subjective Cognitive Decline: Mapping Functional and Structural Brain Changes—A Combined Resting-State Functional and Structural MR Imaging Study." *Radiology* 281, no. 1: 185–192.

Ten, K. M., A. Redolfi, E. Peira, et al. 2018. "MRI Predictors of Amyloid Pathology: Results From the EMIF-AD Multimodal Biomarker Discovery Study." *Alzheimer's Research & Therapy* 10, no. 1: 100.

Thomas, K. R., K. J. Bangen, A. J. Weigand, et al. 2020. "Objective Subtle Cognitive Difficulties Predict Future Amyloid Accumulation and Neurodegeneration." *Neurology* 94, no. 4: 8838.

Tibshirani, R., M. Saunders, S. Rosset, J. Zhu, and K. Knight. 2005. "Sparsity and Smoothness via the Fused Lasso." *Journal of the Royal Statistical Society. Series B, Statistical Methodology* 67, no. 1: 91–108.

Tibshirani, R. J. 1996. "Regression Shrinkage and Selection via the Lasso." *Journal of the Royal Statistical Society, Series B: Statistical Methodology* 58, no. 1: 267–288.

Tosun, D., D. Veitch, P. Aisen, et al. 2021. "Detection of β-Amyloid Positivity in Alzheimer's Disease Neuroimaging Initiative Participants With Demographics, Cognition, MRI and Plasma Biomarkers." *Brain Communications* 3, no. 2: fcab008.

Wang, X., W. Huang, L. Su, et al. 2020. "Neuroimaging Advances Regarding Subjective Cognitive Decline in Preclinical Alzheimer's Disease." *Molecular Neurodegeneration* 15, no. 1: 55.

Wu, H., Y. Song, X. Yang, et al. 2023. "Functional and Structural Alterations of Dorsal Attention Network in Preclinical and Early-Stage Alzheimer's Disease." *CNS Neuroscience & Therapeutics* 29, no. 6: 1512–1524.

Yang, L., Y. Yan, Y. Wang, et al. 2018. "Gradual Disturbances of the Amplitude of Low-Frequency Fluctuations (ALFF) and Fractional ALFF in Alzheimer Spectrum." *Frontiers in Neuroscience* 12: 975.

Zang, Y., T. Jiang, Y. Lu, Y. He, and L. Tian. 2004. "Regional Homogeneity Approach to fMRI Data Analysis." *NeuroImage* 22, no. 1: 394–400.

Zhang, Q., Q. Wang, C. He, et al. 2021. "Altered Regional Cerebral Blood Flow and Brain Function Across the Alzheimer's Disease Spectrum: A Potential Biomarker." *Frontiers in Aging Neuroscience* 13: 630382.

Zhang, Z., L. Cui, Y. Huang, Y. Chen, Y. Li, and Q. Guo. 2021. "Changes of Regional Neural Activity Homogeneity in Preclinical Alzheimer's Disease: Compensation and Dysfunction." *Frontiers in Neuroscience* 15: 646414.

Zhao, Q., Q. Guo, and Z. Hong. 2013. "Clustering and Switching During a Semantic Verbal Fluency Test Contribute to Differential Diagnosis of Cognitive Impairment." *Neuroscience Bulletin* 29, no. 1: 75–82.

Zhao, Q., Q. Guo, F. Li, Y. Zhou, B. Wang, and Z. Hong. 2013. "The Shape Trail Test: Application of a New Variant of the Trail Making Test." *PLoS One* 8, no. 2: e57333.

Zhao, Q., Q. Guo, X. Liang, et al. 2015. "Auditory Verbal Learning Test Is Superior to Rey-Osterrieth Complex Figure Memory for Predicting Mild Cognitive Impairment to Alzheimer's Disease." *Current Alzheimer Research* 12, no. 6: 520–526.

Zhuang, X., D. Cordes, A. R. Bender, et al. 2024. "Classifying Alzheimer's Disease Neuropathology Using Clinical and MRI Measurements." *Journal of Alzheimer's Disease* 100, no. 3: 843–862.